

DCT BASED REGION LOG-TIEDRANK COVARIANCE MATRICES FOR FACE RECOGNITION

Cong Jie Ng, Andrew Beng Jin Teoh, Cheng Yaw Low

School of Electrical and Electronic Engineering, College of Engineering
Yonsei University, Seoul, South Korea

ABSTRACT

Gabor-based region covariance matrix (GRCM) has been demonstrated as a promising descriptor for face recognition. However, GRCM requires large number of filters to achieve satisfactory performance. Furthermore, complex-valued Gabor filters require double convolution operations for each filter that makes the computation more expensive. To alleviate the problem, we propose to adopt real-valued discrete cosine transform (DCT) as filter bank in place of complex-valued Gabor filter. DCT as an orthogonal transform however decorrelates the signal, leads to most energies fall into the diagonal entries of the constructed covariance matrix, which is ill-formed for RCM. We demonstrate that applying non-linear operation on the DCT filter responses ameliorates the decorrelated filter responses effects. Apart from that, while RCM offers spatial information that is useful for recognition tasks, overly small RCM region renders poor covariance estimation, which can affect the recognition performance drastically. In this paper we also propose Log-TiedRank to mitigate the potential undersampling effect suffered by covariance matrix estimation. From the experiments Log-TiedRank shows surprising performance boost over AIRM and Log-Euclidean metric especially when both gallery set and probe set have very different distributions.

Index Terms—DCT, Region Covariance Matrices, Log-TiedRank, Face Recognition.

1. INTRODUCTION

Regional covariance matrix (RCM) is first introduced by Tuzel et al. [1] as a powerful means to fuse multiple correlated image cues or features (e.g., pixel location, intensity, image derivatives, etc.) for object detection and texture classification tasks. In face recognition, Gabor filter responses have been shown favorable in constructing RCM and dubbed Gabor RCM (GRCM) [2]. The promising performance of the original GRCM that uses filter response magnitude leads to proposal of different variants of GRCM such as fusion of Gabor phase and magnitude, Gabor log phase and magnitude, weighted GRCM, kernel GRCM and fusion of Gabor and Local Binary Pattern (LBP) [3]–[8].

Nevertheless, while Gabor filter offers flexibility to extract different orientation features at multi-scale and multi-orientation, tuning the right parameter could be difficult. It is also computational expensive that it requires not only convolving both real and imaginary part of the filter; it is typically configured with a total of 40 filters (i.e., 8 orientations and 5 scales). To circumvent the above mentioned problems, we propose to adopt real-valued DCT as filter bank (i.e., half of the Gabor filter convolution

operations). This technique however yields decorrelated filter responses that are not suitable for RCM construction. In section 3 we demonstrate that applying a nonlinear operation on the filter responses can alter the filter responses characteristic for better RCM construction.

Furthermore, despite RCM capability of implicitly encoding spatial information of an image region, estimating a good covariance requires a large number of derived features. An image region is usually very small in which the number of derived features may not be enough to estimate a reliable covariance especially when the probe set and gallery set have very different distributions (e.g., face pose and occlusions). To address this problem, we propose a method called Log-TiedRank. Specifically, we first flatten the manifold where a DCT based RCM resides and then the resulting vector is sorted with tied-rank criterion to obtain the final feature vector for recognition.

Lastly, we provide extensive experiment results with a number of benchmark face datasets to evaluate the effectiveness of the proposed DCT as filter bank and Log-TiedRank in comparison to other methods.

2. PRELIMINARY

RCM proposed by Tuzel et al. [1] uses covariance as a region descriptor to encode multiple image cues and extracted features from image $I \in \mathbb{R}^{n \times m}$ for recognition task. The image cues or extracted features such as pixel location, intensity, and filter responses are described with a mapping function $z_i = \phi(I, x, y) \in \mathbb{R}^d, 0 \leq i < nm$. Where x, y are the pixel location and d is the feature map dimension that forms a $d \times d$ covariance matrix, \mathbf{C} for an image region.

$$\mathbf{C} = \frac{1}{N} \sum_{i=1}^N (z_i - u)(z_i - u)^T, \quad (1)$$

where u is the mean of z and N is the number of samples of a region. A covariance matrix is a symmetric positive definite (SPD) matrix that lies on Riemannian Manifold where applying Euclidean metric directly often leads to swelling effects [9]. Instead, geodesic distant induced by Riemannian metric is used for measuring similarity between two SPD matrices C_1 and C_2 . In this paper, we choose the following two metrics as baseline for evaluating our proposed method:

(a) **Affine Invariant Riemannian Metric (AIRM)** [10]

$$d(C_1, C_2) = \sqrt{\sum_{i=1}^n \ln^2 \lambda_i(C_1, C_2)} \quad (2)$$

where $\lambda_i(C_1, C_2)$ is generalized eigenvalues of C_1 and C_2

(b) **Log-Euclidean Distance (Log-Euc)** [9]

$$d(C_1, C_2) = \|\text{Log}(C_1) - \text{Log}(C_2)\|_F \quad (3)$$

where $\text{Log}(\cdot)$ is matrix logarithm, and F is Frobenius norm.

3. DCT AS FILTER BANK FOR REGION COVARIANCE MATRIX

An image is typically locally correlated in spatial domain in which one can predict the neighbor sample of a particular spatial location with high confidence. However, it is no longer the case when the image is transformed with orthogonal transform such as DCT [11]. The transformed or decorrelated feature provides little information about the correlation between its neighbors. Consequently, the covariance matrix of the decorrelated features would have most energies concentrated in the diagonal entries while the off diagonal entries energy would be relatively small.

Although in this work DCT is used as a filter bank, convolving a $k \times k$ size DCT basis with an image can also be viewed as projecting overlapped (i.e., stride one) local images of patch size $k \times k$ onto the DCT basis. Except that projection does not flip the basis as convolution does, both are equivalent for symmetric filters. In other words, with the flipped image patch, projection is also equivalent to convolution. Hence, convolving an image with DCT filters that inherits the decorrelation characteristic is not suitable for RCM construction.

In order to adopt DCT as filter bank for RCM, we apply non-linear operation (e.g., modulus, squarer, etc) on the filter responses to break the decorrelation between filter responses. Fig 1 illustrates that applying modulus operation on the filter responses turns the decorrelated filter responses (i.e., energies are concentrated only in diagonal entries) to be globally correlated (i.e., energies spread to off diagonal entries). The filter responses are obtained by convolving a face image with a total of $49 \times 7 \times 7$ DCT filters. This in turn increases the covariance matrix discriminant capabilities by encoding more correlated information among the features.

Lastly, to decrease even more computation, we select only a subset with T number of bases from DCT as filter bank. In this work we adopt the basis selection method proposed by DCTNet [12] which ranks the bases based on horizontal-frequency major scanning order with the intuition that distinct human face features compose of more high frequency horizontal components. The first filter obtained from the scanning order is DC component of DCT. However, omitting the DC component that acts as the means of an image patch provides robustness to the extracted feature against illumination variations. Therefore, the basis selection index is from 2 to $T + 1$.

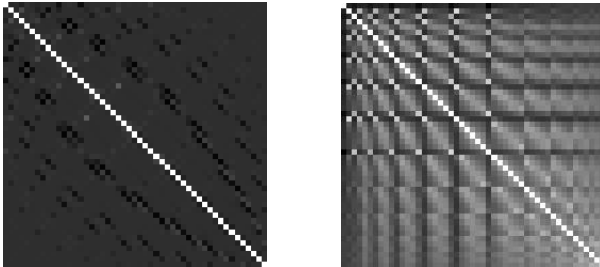


Fig 1: For illustration purposes normalized covariance matrix (i.e., correlation matrix) is used. Left shows the obtained covariance matrix without non-linear operation, right shows the obtained covariance matrix with absolute operation.

4. REGIONAL LOG-TIEDRANK COVARIANCE MATRIX (RLTCM)

Regional covariance matrix (RCM) [1] is capable of implicitly capturing spatial information by encoding local image region with covariance matrix. Spatial information is found to be useful for some recognition tasks like face recognition to encode face feature information separately in their respective region [2], [13]. While smaller region gives better spatial information precision, the covariance estimation gets poorer. It is also known that sample covariance matrix is very sensitive to outliers [14]. With a small number of samples an outlier can give bigger impact on the computed covariance matrix. Furthermore, estimating a good covariance matrix for representing an image region is essential for good recognition performance especially when the probe set distribution is far deviated from the gallery set (e.g., face with different pose). Extracting features that are very different from the gallery set can degrade the performance significantly.

One possible solution to the above mentioned problems is to replace covariance matrix with Spearman’s rank correlation matrix [15] which computes Pearson correlation among ranked variables. It works by eliminating disparity between samples hence more robust against undersampling and outliers, but this solution involves heavy computation. Rather than adopting Spearman’s rank correlation matrix as the solution¹, we opt to regulate the covariance matrix directly. However, regulating a non-singular covariance matrix is not trivial as it is a symmetric positive definite (SPD) matrix that lies on a Riemannian manifold [10]. Instead, we embed the nonsingular covariance matrix, $S \in \mathbb{R}^{n \times n}$ into its tangent space with respect to origin (identity matrix, I) to form a symmetric matrix, $S' \in \mathbb{R}^{n \times n}$ with principal matrix logarithm² in vector space [9].

$$S' = \text{Log}_t(S) \quad (4)$$

To simplify the computation, either part of the off diagonal entries of S' can be omitted. Then, the remaining off diagonal entries are multiplied by $\sqrt{2}$ to compensate the loss energy. After vectorization, we obtain $S' \cong \vec{S}' \in \mathbb{R}^m$ [16]:

$$\vec{S}' = [S'_{1,1}, \sqrt{2}S'_{1,2}, \sqrt{2}S'_{1,3}, \dots, \sqrt{2}S'_{n,n-2}, \sqrt{2}S'_{n,n-1}, S'_{n,n}]^T \quad (5)$$

where $m = \frac{n(n+1)}{2}$ and $S'_{i,j}$ is the coefficient of S' at (i, j)

With \vec{S}' in vector space, we adopt the tied rank principle inspired by Spearman’s rank correlation [15] to represent \vec{S}' and we obtain $\vec{v} = \text{TR}(\vec{S}')$ where $\text{TR}(\vec{x})$ is a function that returns rank order of each element of \vec{x} in ascending order. Average rank is assigned to all elements that are tied in rank order. Finally, \vec{v} is used to represent the image region. Rank representation is able to not only eliminate disparity among features, it can also represent vectors that have the same rank order but different scales with an exact same representation, making it more robust than actual value representation when both probe set and gallery set are far deviated.

¹ We have tested replacing covariance matrix with Spearman’s rank correlation matrix. Even though it gives recognition performance gain, our proposed Log-TiedRank gives better performance and it has much lower computation complexity.

² Note that $\text{Log}_t(S)$ is not the scalar \log function, it is the principal matrix logarithm that always exist a unique real and symmetric logarithm when S is SPD.

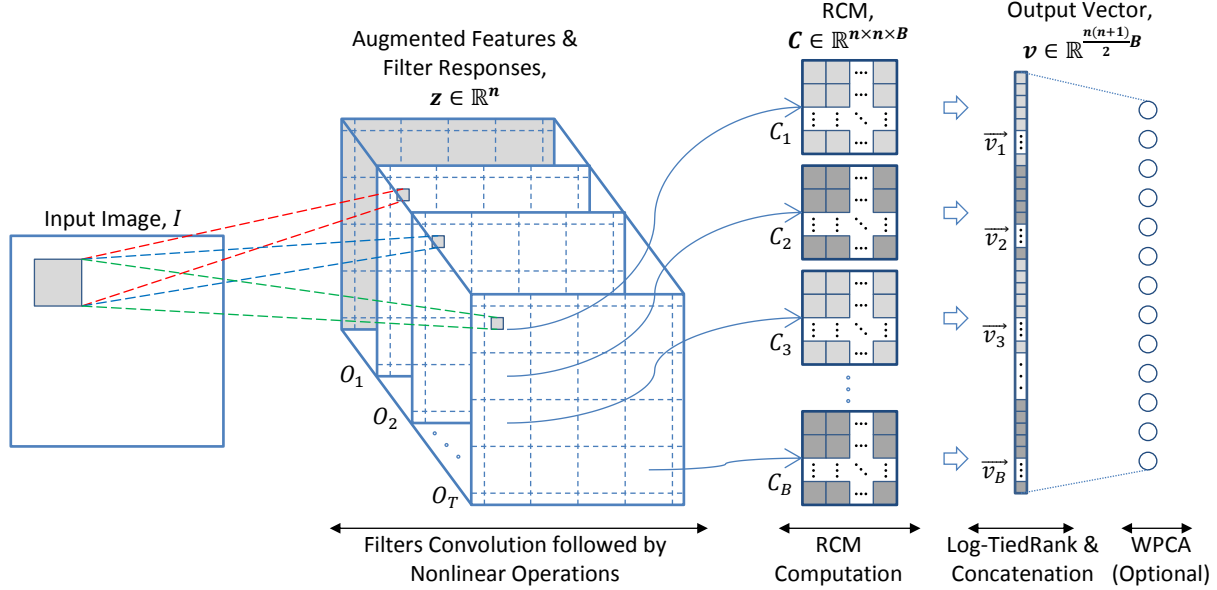


Fig 2 : Block diagram of the feature extraction pipeline

5. FEATURE EXTRACTION PIPELINE

Given an input image I , and a set of filters H that consists of T filters with filter size $k \times k$ each. Boundary of I is zero padded with pad size $(k - 1)/2$ to keep the output filter response size the same as input image size. Convolution of H with I yields T filter responses. These responses are then normalized to unit variance and zero mean. Followed by square rooting the absolute value of the normalized responses forms

$$O_i = \sqrt{\frac{|(I * H_i) - \mu|}{\sigma}}, i = 1, \dots, T \quad (6)$$

where μ and σ are the filter responses mean and standard deviation respectively. To increase the discriminant capabilities as proposed by the original RCM work [1], image pixel coordinate is added as an augmented feature into z to form the final feature mapping function

$$z(x, y) = [x, y, O_1(x, y), \dots, O_T(x, y)]^T \quad (7)$$

Where x and y are image pixel coordinates. To form RCM, z is partitioned into B non-overlapping regions of size $l_1 \times l_2$ each and covariance matrix of all the regions are obtained denoted by $C \in \mathbb{R}^{n \times n \times B}$, where $n = T + 2$. Then, Log-TiedRank is performed on each i^{th} covariance matrix C_i to obtain $\vec{v}_i \in \mathbb{R}^{\frac{n(n+1)}{2}}$. Concatenating all \vec{v}_i forms the final vector of the input image I

$$\mathbf{v} = [\vec{v}_1^T, \vec{v}_2^T, \vec{v}_3^T, \dots, \vec{v}_B^T]^T \in \mathbb{R}^{\frac{n(n+1)}{2}B} \quad (8)$$

Lastly, the dimension of \mathbf{v} can be reduced optionally with whitening PCA (WPCA) where the projection matrix is learned from gallery set.

6. EXPERIMENTS AND DISCUSSIONS

In this section, we evaluate the effectiveness of the proposed DCT as filter bank and Log-TiedRank on 3 benchmark face datasets namely AR [17], FERET-I (subset ‘b’) and FERET-II (‘fa’, ‘fb’),

‘fc’, ‘dup-I’ and ‘dup-II’) [18] with rank-1 recognition rate. For comparison, we also apply Gabor filter into our feature extraction pipeline without non-linear operation as the magnitude of the filter responses is already positive value. Then, the robustness of Log-TiedRank (Log-TR) is evaluated by comparing with Affine Invariant Riemmanian Metric (AIRM) [10] and Log-Euclidean distant (Log-Euc) [9] as baseline. Lastly, Nearest Neighbor classifier is used on all the experiments and cosine distant is applied on Log-TiedRank method.

The same parameters are used throughout all the experiments except for the RCM size. For DCT we set the filter size $k \times k$ as 11×11 with a total number of filters, $T = 30$. Whereas for Gabor filter we use 40 filters (i.e., $u = \{0, 1, \dots, 7\}$, $v = \{0, 1, \dots, 4\}$) of size 11×11 and the rest are tuned to $kmax = \pi/2$, $f = \sqrt{1.8}$, $\sigma = \pi$.

6.1. Evaluation on AR Dataset

TABLE I: AR RECOGNITION RATES (%)

Filter	Metric	Expres.	Illum.	Occlus.	Avg
Gabor	AIRM [2]	97.643	99.663	92.845	96.717
	Log-Euc	94.781	96.465	82.828	91.358
	Log-TR	99.327	100	99.327	99.551
DCT	AIRM	98.822	98.990	93.014	96.942
	Log-Euc	97.980	98.148	85.606	93.911
	Log-TR	98.485	99.832	98.317	98.878

We first evaluate with AR dataset [17] which consists of over 4000 images allows us to evaluate our method against face expression changes, illumination variations and occlusions. In the experiment, the dataset is converted to grayscale and cropped to 165×120 . Out of 126 subjects, we use subset of 50 males and subset of 50 females. Then, 2 frontal faces with neutral facial expression are used as gallery set and the rest are used as probe set which are divided into 3 groups namely expression, illumination and occlusion. Lastly, the region size of RCM $l_1 \times l_2$ is set to 20×20 .

From Table I, it is observed that both filters are robust against expression changes due to the reason that RCM itself provides some deformation tolerances at local region. Besides that, Gabor

filter that extracts only directional features and DCT filter choice that omits DC component (i.e., local image patch average intensity) make them robust against illumination variations. Lastly, while both filters have slightly poor performance against occlusions with AIRM and Log-Euclidean metric, Log-TiedRank that is robust against outliers (i.e., occluded area) shows significant performance gain.

6.2. Evaluation on FERET-I

TABLE II : FERET-I RECOGNITION RATES (%)

Filter	Metric	Bc	Bd	Be	Bf	Bg	Bh	Avg
Gabor	AIRM [2]	50.5	94.0	99.0	99.0	88.5	48.0	79.83
	Log-Euc	45.0	86.0	97.5	98.0	83.5	43.5	75.58
	Log-TR	81.5	99.5	99.5	100	96.5	76.0	92.17
DCT	AIRM	61.0	94.5	99.5	99.5	94.5	70.0	86.50
	Log-Euc	52.5	89.0	99.0	99.5	91.5	62.5	82.33
	Log-TR	94.5	100	100	100	99.0	89.0	97.08

Next, we evaluate our proposed method with FERET ‘b’ subset [18]. It consists of 200 subjects with a total of 1800 images. Each image is aligned with eyes and mouth and resized to 128×128 . In the experiment, frontal faces with expression and illumination (i.e., Ba, Bj and Bk) are used as gallery set and non-frontal face (i.e., Bc, Bd, Be, Bf, Bg, Bh) are used as probe set with the pose range from +40 to -40 degree. For this dataset, RCM size $l_1 \times l_2$ is set to 20×20 .

Based on Table II while both Gabor and DCT have poor performance on Bc and Bh (i.e., +40 and -40 degree pose respectively), DCT remarkably outperforms Gabor for all metrics. DCT extracts features that are based on horizontal and vertical frequency band is less sensitive to local rotation than Gabor filter that extracts u orientations (i.e., $u = \{0, 1, \dots, 7\}$ in this experiment). A slight orientation change can greatly affect the Gabor filter extracted features.

As oppose to AIRM and Log-Euclidean which use actual value representation, Log-TiedRank that uses rank representation is insensitive to precision difference can represent both gallery set and probe set that are far deviated with less deviated representations. With this reason, Log-TiedRank shows huge performance gain on Bc and Bh probe sets that are far deviated from the frontal face gallery set.

6.3. Evaluation on FERET-II

TABLE III : FERET-II RECOGNITION RATES (%)

Filter	Metric	Fb	Fc	Dup-I	Dup-II	Avg
Gabor	AIRM [2]	91.72	93.30	61.77	63.25	77.51
	Log-Euc	87.11	85.05	53.60	51.28	69.26
	Log-TR	95.90	99.48	76.18	73.93	86.37
	Log-TR+WPCA	99.41	100	91.55	91.45	95.60
DCT	AIRM	93.72	95.36	68.56	70.94	82.15
	Log-Euc	92.47	93.30	61.63	63.25	77.66
	Log-TR	96.99	99.48	81.86	83.76	90.52
	Log-TR+WPCA	99.33	100	92.80	92.31	96.11

Lastly, FERET [18] with subset Fa, Fb, Fc, Dup-I and Dup-II are used for evaluation. Each subset consists of 1196, 1195, 194, 722 and 234 subjects respectively. In the experiment, each grayscale image is resized and cropped to 128×128 . We use Fa as gallery set and the rest are used as probe set. Then we set RCM region size $l_1 \times l_2$ to 16×16 .

The experiment results from Table III show that DCT outperforms Gabor for all methods. It also shows that Log-TiedRank consistently shows significant performance gain especially on Dup-I and Dup-II that consist of aged faces. To have even better recognition performance, we also apply Whitening PCA (WPCA) after Log-TiedRank stage as shown in Fig 2. The WPCA projection matrix is learnt from Fa gallery set and it is reduced to 1000 dimension.

6.4. Comparison with other RCM based methods

TABLE IV : COMPARISON WITH OTHER RCM BASED METHODS

Method	Fb	Fc	Dup-I	Dup-II	Avg
RCM [1]	85.19	27.84	44.04	29.06	46.53
Sigma Sets [19]	89.62	91.75	50.55	44.87	69.20
GRCM [2]	91.72	93.30	61.77	63.25	77.51
GWRCM [6]	91.63	93.30	62.19	64.10	77.81
DCT (AIRM)	93.72	95.36	68.56	70.94	82.15
DCT (Log-TR + WPCA)	99.33	100	92.80	92.31	96.11

For comparison, we also evaluate other RCM based methods with our pipeline (without non-linear operations and Log-TiedRank) except for Sigma Sets, input image and filter responses are normalized to zero mean and unit variance. We follow the AIRM [10] metric used by RCM [1], GRCM [2] and GWRCM [6] and Modified Hausdroff Distance [20] used by Sigma Sets [19]. For RCM, mapping function is set to $z(x, y) = \left[x, y, I(x, y), \frac{\partial I(x, y)}{\partial x}, \frac{\partial I(x, y)}{\partial y}, \frac{\partial^2 I(x, y)}{\partial x^2}, \frac{\partial^2 I(x, y)}{\partial y^2} \right]^T$, and for the rest, the same $z(x, y)$ from the previous experiments are used. Lastly, the σ parameter of the GWRCM similarity function (i.e., Gaussian function) is set to $\sigma = 70$.

From Table IV despite simplicity both our proposed DCT as filter bank on RCM that uses AIRM metric as baseline and Log-TiedRank with WPCA show superior performance among all the compared RCM based methods.

7. CONCLUSION

To conclude, with a simple nonlinear operation we are able to make the decorrelated filter responses obtained from DCT to be globally correlated making it suitable for RCM construction. From the experiments, we also demonstrate that despite low complexity the real-valued DCT with 30 filters which requires less than half of the convolution operations outperforms complex-valued Gabor with 40 filters in most cases. It is also shown that, DCT is more robust against occlusions and pose changes. In the case where the constructed RCM from probe set is far deviated from gallery set, it can drastically affect the recognition performance. With Log-TiedRank that represents the flatten RCM manifold vector with rank order makes the extracted features from probe set and gallery set less deviated from each other proves useful.

8. ACKNOWLEDGEMENT

This work was supported by Basic Science Research Program through the National Research Foundation of Korea (NRF) funded by Ministry of Science, ICT and Future Planning (2013006574) and Institute of BioMed-IT, Energy-IT and SmartIT Technology (BEST), a Brain Korea 21 Plus Program, Yonsei University.

9. REFERENCES

- [1] O. Tuzel, F. Porikli, and P. Meer, "Region Covariance: A Fast Descriptor for Detection and Classification," in *Computer Vision – ECCV 2006*, A. Leonardis, H. Bischof, and A. Pinz, Eds. Springer Berlin Heidelberg, 2006, pp. 589–600.
- [2] Y. Pang, Y. Yuan, and X. Li, "Gabor-Based Region Covariance Matrices for Face Recognition," *IEEE Trans. Circuits Syst. Video Technol.*, vol. 18, no. 7, pp. 989–993, Jul. 2008.
- [3] J. Lu, Y. Zhao, and J. Hu, "Enhanced gabor-based region covariance matrices for palmprint recognition," *Electron. Lett.*, vol. 45, no. 17, pp. 880–881, Aug. 2009.
- [4] M. Mu and Q. Ruan, "Region covariance matrices as feature descriptors for palmprint recognition using gabor features," *Int. J. Pattern Recognit. Artif. Intell.*, vol. 25, no. 04, pp. 513–528, Jun. 2011.
- [5] Y. Zhang and S. Li, "Gabor-LBP Based Region Covariance Descriptor for Person Re-identification," in *2011 Sixth International Conference on Image and Graphics (ICIG)*, 2011, pp. 368–371.
- [6] H. F. Qin, L. Qin, L. Xue, and C. B. Yu, "Gabor-based weighted region covariance matrix for face recognition," *Electron. Lett.*, vol. 48, no. 16, pp. 992–993, Aug. 2012.
- [7] H. Qin, L. Qin, L. Xue, and Y. Li, "A Kernel Gabor-Based Weighted Region Covariance Matrix for Face Recognition," *Sensors*, vol. 12, no. 6, pp. 7410–7422, May 2012.
- [8] Y. Pang, Y. Yuan, and X. Li, "Effective Feature Extraction in High-Dimensional Space," *IEEE Trans. Syst. Man Cybern. Part B Cybern.*, vol. 38, no. 6, pp. 1652–1656, Dec. 2008.
- [9] V. Arsigny, P. Fillard, X. Pennec, and N. Ayache, "Geometric Means in a Novel Vector Space Structure on Symmetric Positive-Definite Matrices," *SIAM J. Matrix Anal. Appl.*, vol. 29, no. 1, pp. 328–347, Jan. 2007.
- [10] X. Pennec, P. Fillard, and N. Ayache, "A Riemannian Framework for Tensor Computing," *Int. J. Comput. Vis.*, vol. 66, no. 1, pp. 41–66, Jan. 2006.
- [11] R. Wang, *Introduction to Orthogonal Transforms: With Applications in Data Processing and Analysis*, 1 edition. Cambridge England; New York: Cambridge University Press, 2012.
- [12] C. J. Ng and A. B. J. Teoh, "DCTNet: A simple Learning-free Approach for Face Recognition," *ArXiv150702049 Cs*, Jul. 2015.
- [13] T. Ahonen, A. Hadid, and M. Pietikainen, "Face Description with Local Binary Patterns: Application to Face Recognition," *IEEE Trans. Pattern Anal. Mach. Intell.*, vol. 28, no. 12, pp. 2037–2041, Dec. 2006.
- [14] W. N. Venables and B. D. Ripley, *Modern Applied Statistics with S*, Fourth. New York: Springer, 2002.
- [15] C. Spearman, "The Proof and Measurement of Association between Two Things," *Am. J. Psychol.*, vol. 15, no. 1, pp. 72–101, Jan. 1904.
- [16] V. Arsigny, P. Fillard, X. Pennec, and N. Ayache, "Log-Euclidean metrics for fast and simple calculus on diffusion tensors," in *Magnetic Resonance in Medicine*, 2006.
- [17] A. M. MARTINEZ, "The AR face database," *CVC Tech. Rep.*, vol. 24, 1998.
- [18] P. J. Phillips, H. Wechsler, J. Huang, and P. J. Rauss, "The FERET database and evaluation procedure for face-recognition algorithms," *Image Vis. Comput.*, vol. 16, no. 5, pp. 295–306, Apr. 1998.
- [19] R. Srinivasan, A. Nagar, A. Tewari, D. Mitrani, and A. Roy-Chowdhury, "Face recognition based on SIGMA sets of image features," in *2014 IEEE International Conference on Acoustics, Speech and Signal Processing (ICASSP)*, 2014, pp. 499–503.
- [20] M.-P. Dubuisson and A. K. Jain, "A modified Hausdorff distance for object matching," in *Proceedings of the 12th IAPR International Conference on Pattern Recognition, 1994. Vol. 1 - Conference A: Computer Vision and Image Processing*, 1994, vol. 1, pp. 566–568 vol.1.